Computational studies on nitratoethylnitramine (NENA), its tautomers and charged forms

Lemi Türker*, Taner Atalar

Middle East Technical University, Department of Chemistry, 06531 Ankara, Turkey

ARTICLE INFO

ABSTRACT

An energetic material, nitratoethylnitramine (NENA), its tautomers and also its charged forms are considered quantum chemically, using various basis sets at the levels of *ab initio* and density functional theories (DFT). NENA has been found to be sensitive to negative charge development, resulting in rupture of O—NO$_2$ bond. Also conformational and molecular dynamics (MD) studies have been performed on NENA. Various geometrical parameters, energies and infrared spectra have been obtained and discussed. Also, calculations indicate that *s-cis* conformation of NENA is slightly more stable than the *s-trans* and the tautomers of it have very comparable total energy values to NENA. On the other hand, on the basis of homolytic bond dissociation energies (BDE) for O—NO$_2$ bond in the structures, it is clear that the presence of the tautomers in the bulk of NENA somewhat should decrease its sensitivity.

© 2008 Elsevier B.V. All rights reserved.

1. Introduction

The prediction of the sensitivity of the energetic materials from molecular structure using molecular orbital and molecular dynamics (MD) studies is an on-going area of research. Recently, many articles appeared in the literature involving quantum chemical computational techniques to investigate various properties of energetic materials [1–7]. Polymer bonded explosives (PBXs) were developed in order to reduce sensitivity of the synthesized explosive crystals by embedding the explosive crystals in a rubber-like polymeric matrix. The first PBX composition was developed at the Los Alamos Scientific Laboratories in USA in 1952. Energetic plasticizers are being used as ingredients in gun and rocket propellants and high explosive compositions. The primary role of energetic plasticizers in energetic material formulations is to modify the mechanical properties of the charge to improve safety characteristics. This is achieved by softening the polymer matrix and making it more flexible by improving certain properties such as tensile strength, elongation, toughness and softening point (Tg point). Energetic plasticizers and binders developed or used during the last decade contain various energetic groups such as nitric acid ester group, nitramine group, azido group, etc. The basic objectives of developing energetic binders and plasticizers are: (a) increase of the thermal stability, (b) increase in energy content, (c) adjust-ment of the oxygen balance in a formulation, (d) improvement of the plasticizer functions in formulations by reducing the glass transition temperature and the brittle–ductile transition temperature, reducing migration and the so-called exudation, improving of other mechanical properties of the propellant matrix and (e) the improvement of the burning behavior of the propellant [8].

One of the well-known and widely used energetic plasticizers is NENA (nitratoethylnitramine (NENA), shown in Fig. 1) type structures. Nitratoethylnitramine possesses an inorganic ester group (nitrato) as well as a nitramine moiety. Presence of these groups and the flexibility of the bonds are responsible for the energetic plasticizer properties of NENA. Although, it is still being used in ammunition industry, lack of information about NENA at the molecular level has encouraged us to perform some quantum chemical studies. Various alkyl NENAs are known and readily manufactured by nitration of commercially available alkylethanolamines, in high yields (80%).
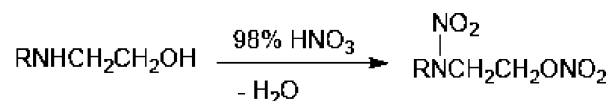
The nitratoethylnitramine family (NENAs) are effective plasticizers in energetic formulations, particularly in nitrocellulosic systems. NENAs contain both nitrate ester (inorganic ester type) and nitramine functionalities. Typical NENA derivatives which are in use include various R groups on amine nitrogen (R = methyl, ethyl, propyl, *iso*-propyl, butyl, and pentyl) [9]. The NENAs have been known since the 1940s, where DINA (dinitroxy ethyl nitramine)
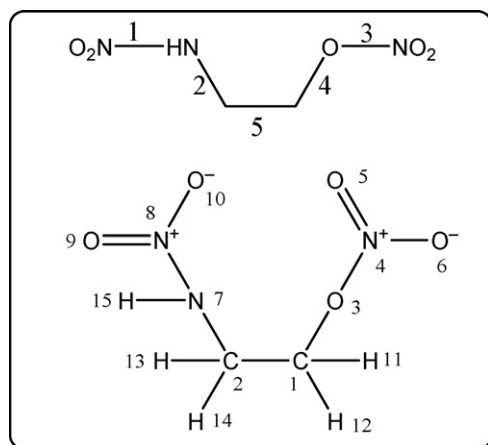
Fig. 1. Numbering of the atoms and bonds of NENA.

was scaled-up for use in Navy flashless gun propellants [10,11]. The use of NENAs as plasticizers in gun and rocket propellants confer excellent properties such as high burning rates, reductions in flame temperature and product gas molecular weight, and higher specific impulse (based on moderate loadings of 60–70% RDX in a nitrocellulose/NENA binder) [12]. NENAs possess good thermal stability, readily plasticize nitrocellulose and other polymers, generate low molecular weight combustion gases, and give good impact sensitivity [9,13].

Alkyl-NENAs are energetic plasticizers produced in industrial quantities based on a Dyno Nobel patented process. The introduction of bu-NENA based gun propellant formulations would allow a better and mechanically improved, energetically enhanced, and less sensitive gun propellant [10–14]. There are some studies concerning their synthesis [15–17] and their explosive properties as insensitive energetic explosives [18–20]. Since its synthesis, alkyl-NENA has been at the center of intense research. The explosive properties of NENA compounds strongly depend on their energetic nitramino and nitrato groups, where the latter are often responsible for an elevated sensitivity and a reduced stability [21]. However, most of the work is in the form of patents, and very little work has been reported in publicly available literature. Although high precision computational chemistry methods have been applied to most successfully for modeling the characteristics of potential high energy (HE) substances [1–7], there has been no computational study about NENA in the literature, to the best of our knowledge. In this study, the neutral and various charged forms of NENA and its tautomers have been considered for their relative stabilities to investigate whether the charged forms play any role in the decomposition or explosion process. Presently, also thermal stabilities have been evaluated from the homolytic bond dissociation energies (BDE) of N—NO$_2$, C—NO$_2$, C—C, C—O, C—N bonds (shown in Fig. 1).

2. Method of calculation

All the calculations for the geometry optimizations and energies were performed using Gaussian 03 program package [22]. The methods used include the UB3LYP/6-311G(d,p), UB3LYP/6-311+G(d,p), UB3LYP/6-311++G(d,p), UB3PW91/6-311G(d,p), MP2/6-311G(d,p)//UHF/6-311G(d,p) and UB3LYP/aug-cc-pVDZ for the calculation of charged forms (+2, +1, 0, −1, −2) [23–25]. In the case of tautomers (T$_1$ and T$_2$) and conformations of NENA (*s-cis-* and *s-trans-*NENA), RB3LYP/6-311+G(d,p) and RB3LYP/6-311++G(d,p)level of calculations were performed. Enthalpies of formation were calculated using a new procedure, termed *T*1,

which is a new computational procedure, that provides heats of formation values within 3 kJ/mol (RMSD) of G3(MP2). It requires an HF/6-31(d) structure and two RI-MP2 energy calculations, the first using the 6-31G(d) basis set and the second using the 6-311++G(2df,2p) set. The large basis set RI-MP2 calculation makes use of dual basis set techniques. An empirical correction based only on molecular weight and formal bond counts replaces the QCISD(T), zero-point energy (ZPE) and temperature correction terms in the G3(MP2) model. This permits accurate thermo chemical calculations for uncharged, closed-shell molecules comprising H, C, N, O, F, S, Cl and Br up to molecular weight of 400 amu [26]. It is several orders of magnitude faster than G3(MP2). In order to calculate heats of formation values, Spartan 06 package programme was used [26]. Also, in order to compare the bond strengths, homolytic bond dissociation energy calculations were performed at the level of UB3LYP/6-311+G(d,p). The homolytic BDE [27,28] is defined for the present case as: BDE = E(X) + E(R) − E(R–X), where E stands for the respective total energy corrected for the zero-point energy for each parent structure and the fragments (R and X) of the low-energy R—X bond scission reaction. Furthermore, the basis set superposition error (BSSE) analyses were carried out with the counterpoise method, introduced by Boys and Bernardi [29]. The corresponding BSSE analyses were performed at the same theoretical levels.

For each set of calculations, vibrational analyses were done (using the same basis set employed in the corresponding geometry optimizations). The normal mode analysis for each structure yielded no imaginary frequencies for the 3N−6 vibrational degrees of freedom, where N is the number of atoms in the system. This indicates that the structure of each molecule corresponds to at least a local minimum on the potential energy surface.

Additionally, constant temperature molecular dynamics (actually quantum dynamics UHF/PM3 calculations) [30] were performed, using starting geometries which were optimized at UB3LYP/6-311G(d,p) level. For the molecular dynamic studies a certain protocol was adopted (consisting of heat time: 1 ps, run time: 20 ps, cool time: 1 ps, step size: 0.0005 ps, start temperature: 0 K, simulation temperature: 700 K, final temperature: 698 K, temperature step: 5 K, bath relaxation time: 0.01 ps). All the molecular dynamics studies were done using Hyperchem 7.5 package program [31].

3. Results and discussion

In the present study, *ab initio* and DFT calculations have been performed using various basis sets. Fig. 1 shows the chemical structure of NENA molecule and numbering of the atoms and bonds.

3.1. Optimized geometries

3.1.1. NENA and its charged forms

Static electricity is a serious problem in the manufacture and storage of explosive materials and considerable understanding and effort are required to control it. It is experimentally well proven fact that free electrons exist in combustion flames and gaseous detonation [32]. In some cases it is possible to quench detonation completely by an applied electric field [33]. The applied electric field causes polarization or ionization of the molecule thus changing properties of the bond even leading to the bond rupture. Thus, charge accumulation and distribution on the molecule become important. However, this phenomenon is highly structure dependent. As indicated for univalent anionic forms of NENA, bond cleavage occurs at O3—N4 bond (see also Table 2 and Fig. 2 above), but only some bond length changes happen in the case of univalent

Table 1
Optimized structural parameters of NENA (r in Å, angles in degrees)

Parameter	B3LYP[b]	UB3LYP[a]	UB3LYP[b]	UB3LYP[c]	UB3PW91[a]	UHF[a]	UHF[b]
r(C1–C2)	1.52	1.52	1.52	1.52	1.51	1.51	1.52
r(C2–N7)	1.46	1.46	1.46	1.46	1.45	1.45	1.45
r(N7–N8)	1.39	1.38	1.38	1.39	1.38	1.36	1.36
r(O3–N4)	1.43	1.42	1.42	1.43	1.42	1.34	1.33
r(C1–O3)	1.45	1.45	1.45	1.45	1.44	1.43	1.43
r(N7–H15)	1.02	1.01	1.01	1.01	1.01	1.00	1.00
α(O3C1C2)	105.3	114.0	114.1	105.3	105.3	105.5	104.1
α(C1C2N7)	109.6	111.6	111.8	109.6	109.4	109.0	107.2
α(C1O3N4)	114.5	116.1	116.3	114.4	114.1	116.6	116.4
α(C2N7N8)	117.8	117.7	117.9	117.8	117.8	117.5	118.3
δ(O3C1C2N7)	62.9	91.1	89.2	62.9	62.9	62.6	176.9
δ(N4O3C1C2)	−179.9	−86.3	−88.2	−179.8	−179.3	179.9	−179.5
δ(C1C2N7N8)	167.1	178.3	−179.5	166.6	167.9	172.5	162.6

 [a] 6-311G(d,p).
 [b] 6-311+G(d,p).
 [c] 6-311++G(d,p).

cationic form. Explosive materials are more prone to such kind of electrical and magnetic effects.

Table 1 lists the optimized structural parameters for the NENA. Unfortunately, in the literature there exists no experimental structural data for this molecule. The gathered data from Hartree–Fock calculations for the bond lengths, are smaller than the respective data for density functional theory calculations. As for the specific bond lengths, the calculated C1—C2 bond in all the calculations is the longest one among the all bonds.

Selected optimized structural parameters of charged forms of NENA are shown in Table 2. Unfortunately, most of the attempts to optimize divalent ionic forms of NENA failed. The optimization of divalent anionic form was succeeded only at the UHF/6-311++G(d,p) level of theory. Obviously, as charge develops the

Table 2
Selected optimized structural parameters of charged forms of NENA (r in Å, angles in degrees)

Parameter	Univalent cation	Neutral	Univalent anion
UB3PW91/6-311G(d,p)			
r(C1–C2)	1.76	1.51	1.55
r(C2–N7)	1.36	1.45	1.45
r(N7–N8)	1.46	1.38	1.35
r(O3–N4)	1.72	1.42	2.16
r(C1–O3)	1.32	1.44	1.36
r(N7–H15)	1.02	1.01	1.03
α(C1O3N4)	114.3	114.1	105.7
α(C2N7N8)	120.9	117.8	119.9
δ(O3C1C2N7)	64.4	62.9	42.4
UHF/6-311G(d,p)			
r(C1–C2)	1.52	1.51	1.51
r(C2–N7)	1.47	1.45	1.44
r(N7–N8)	1.48	1.36	1.43
r(O3–N4)	1.37	1.34	1.31
r(C1–O3)	1.42	1.43	1.45
r(N7–H15)	1.02	1.00	1.00
α(C1O3N4)	116.5	116.6	117.1
α(C2N7N8)	123.7	117.5	110.9
δ(O3C1C2N7)	48.6	62.6	70.4
UB3LYP/6-311++G(d,p)			
r(C1–C2)	1.82	1.52	1.55
r(C2–N7)	1.36	1.46	1.46
r(N7–N8)	1.47	1.39	1.35
r(O3–N4)	1.75	1.43	2.24
r(C1–O3)	1.31	1.45	1.37
r(N7–H15)	1.02	1.01	1.02
α(C1O3N4)	114.6	114.4	104.9
α((C2N7N8)	121.1	117.8	120.4
δ(O3C1C2N7)	64.1	62.9	45.7

optimized geometry changes. As seen in Table 2, as the charge develops, certain bonds are elongated or contracted as compared to the neutral structure. Although as compared to neutral form, a moderate change occurred in the C1—C2 bond length of the univalent anion, a rather striking elongation happened in the case of the univalent cation (see Table 2). The univalent cation formation causes mainly the elongation of C1—C2 and N3—N4 bonds. On the other hand, the univalent cation formation causes contraction of C1—O3 bond but elongation of O3—N4 bond which indicates that electron depletion of the structure in the cationic form is mainly on the ester (inorganic ester) oxygen. Consequently, positive charge repulsion between O3 and N4 atoms elongates the respective bond length. These results are consistent with all different levels of calculations performed. As for the univalent anionic species, DFT calculations yield a drastic change for O3—N4 bond length (O—NO$_2$). The univalent anion formation causes elongation mainly O3—N4 bond (2.160 Å at UB3PW91/6-311G(d,p) and 2.237 Å at UB3LYP/6-311++G(d,p)). Note that the univalent anionic form considered actually stands for a dissociated molecule. In other words, it is a system of fragments or hypothetical molecule having a very elongated bond. Whereas, C1—O3 bond is contracted as a result of dissociation. Note that both in the cation and anion formations O3—N4 bond undergoes elongation but in the later case a drastic elongation occurs leading to rupture of the bond. On the other hand, the results indicate that the nitramine part of the molecule is much less sensitive to charge development. All these give some strong clue that any explosion process due to electrical charging commences at the nitrato grouping and NENA is much more sensitive to negative electric charges than the positive charging. Fig. 2 shows the geometry optimized structures of the neutral and charged forms of NENA calculated at UB3LYP/6-311G(d,p) level.

3.1.2. The tautomers

One of the important processes occurring during detonation of high-energetic nitro compounds is tautomerism, which involves the transfer of a hydrogen either by unimolecular 1,3- or 1,5-shift or by a bimolecular process where the transfer occurs intermolecularly [34]. This hydrogen shift results in *aci*-nitro compounds, which dissociate by release of energy to give smaller fragments. Tautomerism competes with many other processes taking place during detonation [34].

The presently considered NENA structure has two tautomeric forms as well which have some resemblance to nitro-*aci* tautomeric forms. Of course some stability differences are expected among them. Presently, these tautomeric forms are called T$_1$ and T$_2$ (*anti* and *syn* forms, respectively, see Fig. 3). Since the tautomeric
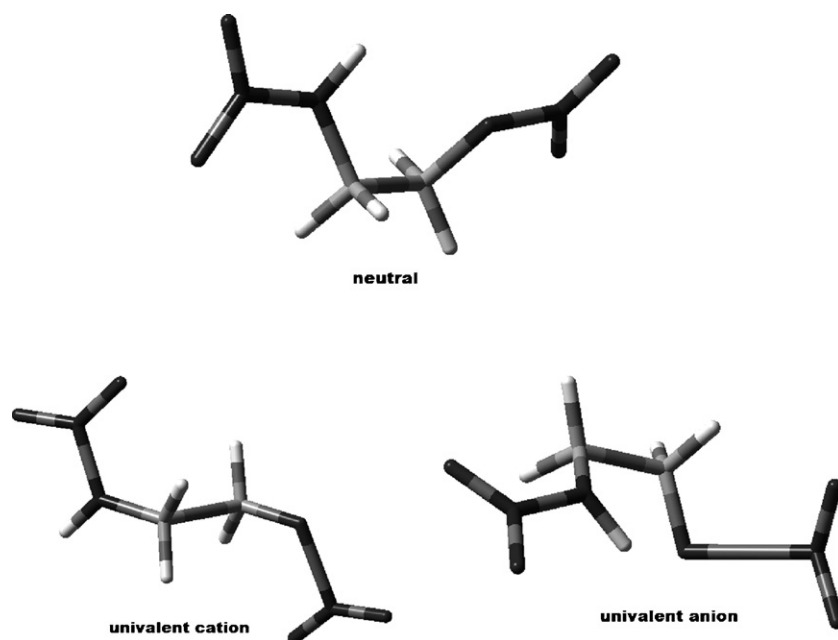
Fig. 2. Geometry optimized structures of the charged forms of NENA calculated at UB3LYP/6-311G(d,p) level (nitramine and nitrato groups are on the left and right, respectively).
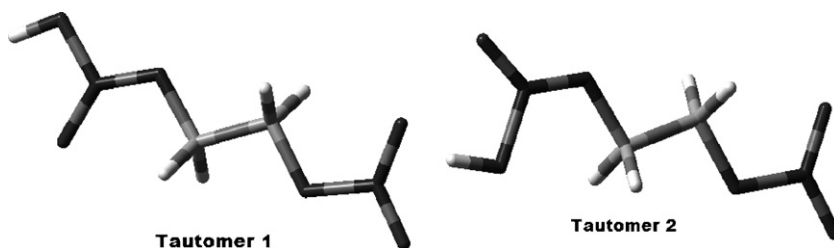

Fig. 3. Geometry optimized structures of the tautomers of NENA. Calculated at B3LYP/6-311+G(d,p) level (nitramine and nitrato groups are on the left and right, respectively).

structures possess lone-pairs and due to the possible hydrogen bondings they might have significant electron density far from the nuclei. Thus, diffuse basis sets have also been used. Fig. 3 shows the geometry optimized structures of the tautomers of present concern. Table 3 lists some geometrical features of the tautomers (B3LYP/6-311+G(d,p)). Numberings of the atoms and bonds are shown in Fig. 1 (the main skeleton of NENA and its tautomers are same, so the same numbering has been used in order to simplify the text). The calculated C1—C2 bond in all the tautomers (T_1, T_2) is longer than that of the NENA considered. The N7–N8 and O3—N4 bonds in the tau-

Table 3
Optimized structural parameters of NENA and its tautomers, T_1 and T_2 (r in Å, angles in degrees) calculated at B3LYP/6-311+G(d,p) level of theory

Parameter	T_1	T_2	NENA
r(C1–C2)	1.52	1.52	1.52
r(C2–N7)	1.46	1.46	1.46
r(N7–N8)	1.25	1.24	1.39
r(O3–N4)	1.42	1.42	1.43
r(C1–O3)	1.44	1.44	1.45
α(O3C1C2)	104.4	104.3	105.3
α(C1C2N7)	106.8	106.2	109.6
α(C1O3N4)	114.3	114.3	114.5
α(C2N7N8)	112.5	117.3	117.8
δ(O3C1C2N7)	180.0	180.0	62.9
δ(N4O3C1C2)	180.0	180.0	−179.9
δ(C1C2N7N8)	180.0	180.0	167.1

tomers are shorter than the corresponding bonds in NENA. Note that N—NO$_2$ and O—NO$_2$ bonds are strengthened in the tautomers (see also Section 3.2 for the bond dissociation energies).

3.2. Energy considerations on species concerned

Besides the charged and tautomeric forms of NENA, some conformers of the concerned molecule have been searched, that is s-cis- and s-trans-NENA conformers are compared (see Fig. 4), and it is found that s-cis-NENA is slightly more stable than the s-trans conformer at the performed calculations (see Table 4). At the level of B3LYP/6-311++G(d,p) level, cis-conformer is 3.4 kJ/mol more stable than the trans-one. Furthermore, the heat of formation values are calculated by using the T1 method (see Table 4) which is a new computational procedure, that provides heats of formation values within 3 kJ/mol (RMSD) of G3(MP2). According to the T1 calculations, again the cis-conformer has been found to be more stable than the trans-one (approximately 11 kJ/mol more stable, see Table 4). These results may reflect that some extent of intramolecular interaction exists to stabilize the cis-conformer over the trans. In the case of cis-conformer, the distance between H15 and O3 atoms, is found to be 2.555 Å by the T1 calculations, however in the case of trans-conformer the same distance is found to be 4.036 Å at the same level of theory. Additionally, based on the geometry optimized structure of NENA at B3LYP/6-311++G(d,p) level of theory, energy profile was screened by changing the dihedral angle δ(O3C1C2N7) from 0° to
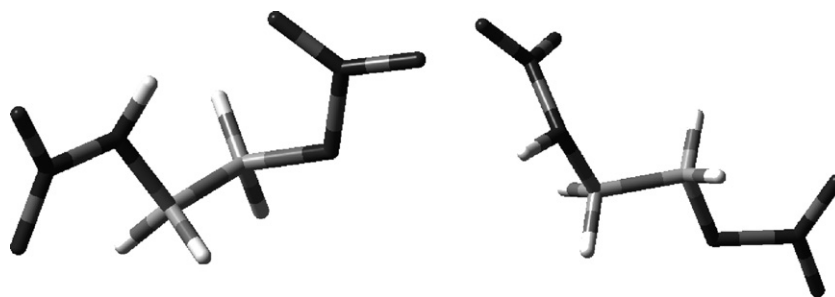
Fig. 4. Geometry optimized structures of the conformers of NENA. Calculated at B3LYP/6-311+G(d,p) level (nitramine and nitrato groups are on the left and right, respectively).

Table 4
Calculated total energies (in hartrees) and heat of formation values (in kJ/mol) of NENA conformers

	B3LYP/6-311+G(d,p)	B3LYP/6-311++G(d,p)	HOF[a]
s-cis-NENA	−619.430739	−619.533189	−75.07
s-trans-NENA	−619.428876	−619.531907	−64.09

[a] Values were obtained from *T*1 calculations.

180° at the level of B3LYP/6-31G(d) (the energy profile calculations were not performed at B3LYP/6-311++G(d,p) level of theory to save time). The results are represented in Table 5 and Fig. 5. As mentioned before, explosive materials are more prone to such kind of electri-
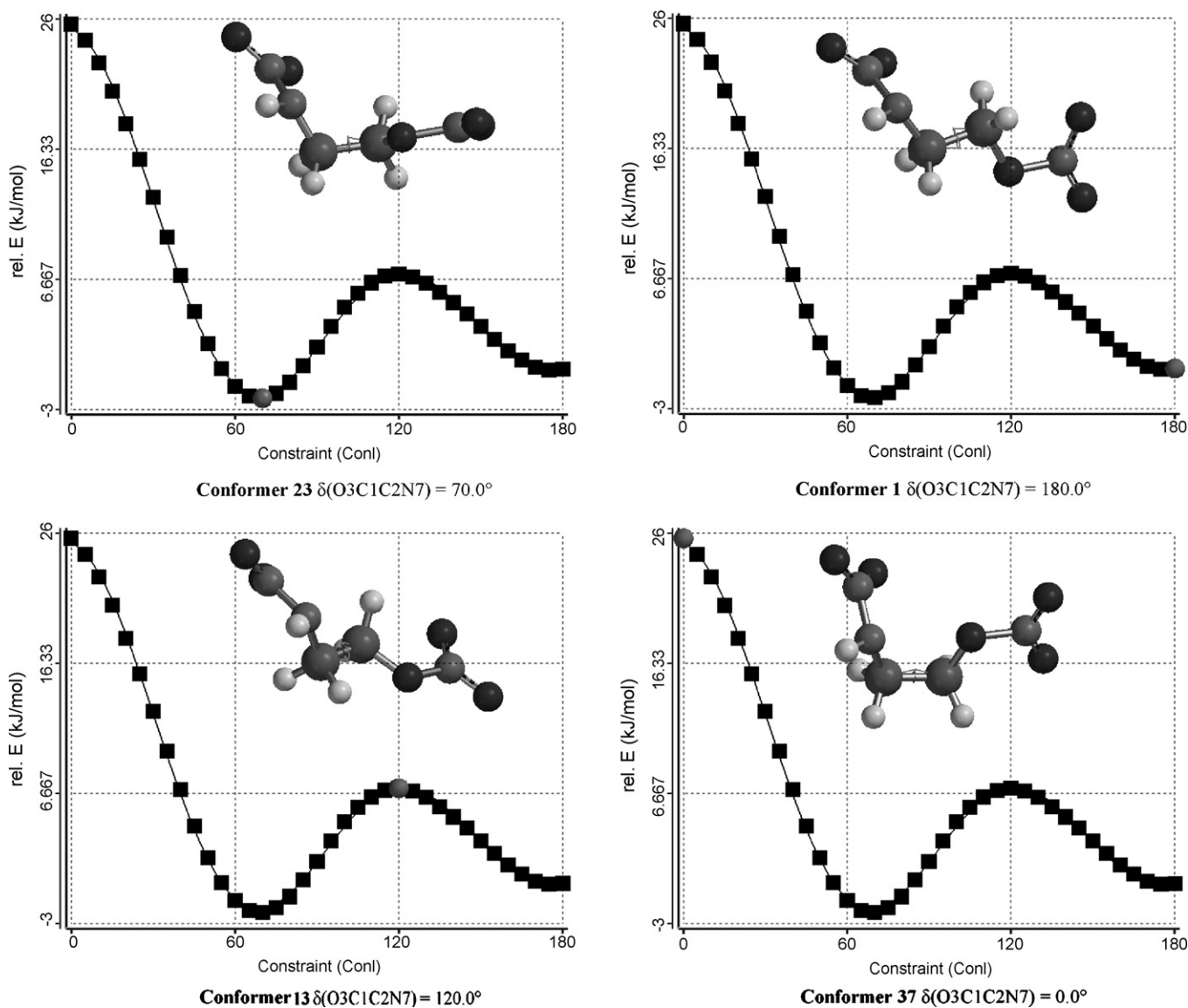
Table 5
Calculated relative energies (kJ/mol) are presented, conformer 1 as the reference structure

Conformers	δ(O3C1C2N7)	Rel. *E* (kJ/mol)
001	180.0	0.000
002	175.0	−0.071
003	170.0	0.161
004	165.0	0.681
005	160.0	1.385
006	155.0	2.215
007	150.0	3.157
008	145.0	4.091
009	140.0	4.926
010	135.0	5.701
011	130.0	6.390
012	125.0	6.870
013	120.0	7.066
014	115.0	6.907
015	110.0	6.403
016	105.0	5.631
017	100.0	4.563
018	95.0	3.173
019	90.0	1.643
020	85.0	0.238
021	80.0	−0.985
022	75.0	−1.803
023	70.0	−2.173
024	65.0	−2.021
025	60.0	−1.271
026	55.0	0.049
027	50.0	1.908
028	45.0	4.283
029	40.0	6.966
030	35.0	9.824
031	30.0	12.748
032	25.0	15.574
033	20.0	18.208
034	15.0	20.638
035	10.0	22.766
036	5.0	24.445
037	0.0	25.618

Initial geometry was optimized at B3LYP/6-311++G(d,p) level and then scanning dihedral angles, energy profile was obtained at B3LYP/6-31G(d) level.

cal and magnetic effects. Hence, their response to such kinds of effects is very important and vital for their manufacturing, storage and handling. The study the charged forms of explosive materials by means of certain quantum chemical methods at the molecular level is very informative for many practical purposes. Table 6 shows some calculated energies of concerned neutral and charged forms of NENA, with zero-point energies are taken into account Recall that in the case of univalent anion, it is not stable structurally (chemically) it stands for the decomposed structure at DFT calculations. As for the tautomers, the stability order is NENA > T_1 > T_2 at all levels of calculations (see Table 7). Furthermore, the calculated heat of formation values (all exothermic) supports the same stability order but highly biasing the NENA structure over the tautomeric forms. Note that in T_2 structure, the oxygen atom bearing the negative charge is aligned (within the limitations of N=N double bond) with the lone-pair of the other nitrogen of the azo group. Whereas in T_1, a similar but less repulsive situation exists with the lone-pair of —OH oxygen and azo nitrogen atom. The above mentioned stability order between the tautomers of NENA arises because of partly electronic factors and partly geometrical ones.

In the literature, the stabilities and impact/shock sensitivities of energetic materials have frequently been related to the strength of C—NO$_2$ and/or N—NO$_2$ bond strengths [4,35]. Also thermal stability of nitramines is mainly related to the energy required for the initial reaction of decomposition [36]. The common initial step of thermal decomposition of nitramines is the NO$_2$ fission reaction through breaking of N—NO$_2$ bond as known in the decomposition of hexahydro-1,3,5-trinitro-*s*-triazine (RDX) and 1,3,5,7-tetranitro-1,3,5,7-tetraazocyclooctane (HMX) [37]. Keeping these in mind, we performed homolytic bond dissociation energies of different bonds of neutral NENA molecule at DFT level. Numbering of bonds are shown in Fig. 1 and homolytic bond dissociation energies and bond lengths of concerned species are shown in Table 8. According to the calculations performed, it is found that the weakest bond is the O—NO$_2$ bond. This indicates the probability of rupture of O—NO$_2$ bond is higher than the nitramine bond (N—NO$_2$). Recall that anionic charge development results in bond rupture of O—NO$_2$ (bond 3 in Table 8). On the other hand, homolytic BDE of this bond is calculated for the tautomers and it is found that this bond is getting stronger in the tautomers compared to NENA (UB3LYP/6-311+G(d,p) level of calculations yield 114, 136 and 126 kJ/mol for NENA, T_1 and T_2, respectively. See Tables 8 and 9). Hence, tautomerism becomes one of the important processes occurring during detonation of energetic materials. In general tautomerism involves the transfer of a hydrogen either by unimolecular 1,3- or 1,5-shift or by a bimolecular process where the transfer occurs intermolecularly [34]. The percentages of tautomers in the bulk affect the sensitivity because the bonding in them might be different than the parent structure. In the light of the present findings, the presence of tautomers makes this energetic material, NENA, more insensitive as compared to the pure form.

Conformer 23 $\delta(O3C1C2N7) = 70.0°$

Conformer 1 $\delta(O3C1C2N7) = 180.0°$

Conformer 13 $\delta(O3C1C2N7) = 120.0°$

Conformer 37 $\delta(O3C1C2N7) = 0.0°$

Fig. 5. Energy profiles are shown, Y-axis is releative energy in units of kJ/mol and X-axis is the dihedral angle of $\delta(O3C1C2N7)$, conformer 1 as the reference structure. Initial geometry was optimized at B3LYP/6-311++G(d,p) level and then energy profile was obtained at B3LYP/6-31G(d). The conformers shown in the graphs are the corresponding geometry of the spherical marks on the energy plots.

Table 6
Calculated total energies, E_0 (including zero-point vibrational energies) of univalent charged forms of NENA at various theoretical levels

	Neutral	Univalent cation	Univalent anion
UB3LYP/6-311G(d,p)	−619.411199	−619.055293	−619.477414
UB3LYP/6-311+G(d,p)	−619.430795	−619.068235	−619.513456
UB3LYP/6-311++G(d,p)	−619.430974	−619.068554	−619.513552
UB3LYP/aug-cc-pVDZ	−619.342202	−618.981438	−619.426105
UB3PW91/6-311G(d,p)	−619.173332	−618.81550	−619.235041
UHF/6-311G(d,p)	−616.155046 (−618.203631)[a]	−615.686726 (−617.961824)[a]	−616.035778 (−618.179638)[a]

[a] The values in parenthesis are single point MP2 energies, calculated after corresponding UHF geometry optimizations. All the values in hartrees.

Table 7
Calculated total energies (in hartrees), E_0 (including zero-point vibrational energies) and heat of formation values (in kJ/mol) of NENA tautomers, T_1 and T_2

	UB3LYP/6-311+G(d,p)	B3LYP/6-311++G(d,p)	UHF/6-311+G(d,p)	HOF[a]
NENA	−619.430739	−619.533189	−616.051671	−75.07
T_1	−619.417136	−619.518909	−616.040959	−44.41
T_2	−619.413550	−619.515072	−616.032704	−40.30

[a] Heat of formation values were obtained from $T1$ method of calculations.

3.3. The frontier orbitals

The frontier molecular orbitals, the HPMP and LUMO, are important in ionization processes. The sensitivity of energetic materials to charge development is mainly dictated by the HOMO and LUMO energies.

Figs. 6 and 7 show the frontier molecular orbitals (the highest occupied and lowest unoccupied molecular orbitals; HOMO and

Table 8
Homolytic bond dissociation energies (in kJ/mol) and bond lengths (Å) of neutral NENA compound (numbering of bonds are shown in Fig. 1)

| Calculation type	Bond				
	1	2	3	4	5
UB3LYP/6-311+G(d,p)	162.9 (1.38)[a]	324.6 (1.46)[a]	114.7 (1.42)[a]	286.8 (1.45)[a]	277.6 (1.52)[a]

[a] The values in parenthesis are bond lengths in Å. BDEs include basis set superposition error (BSSE) and zero-point energy (ZPE) corrections.

Table 9
Homolytic bond dissociation energies (in kJ/mol) of O—NO_2 bond in tautomers T_1 and T_2

Calculation type	Tautomer	
	T_1	T_2
UB3LYP/6-311+G(d,p)	136	126

BDEs include basis set superposition error (BSSE) and zero-point energy (ZPE) corrections.

LUMO, respectively) of the neutral and charged forms of NENA. In the case of neutral structure, both the α- and β-HOMO arise mainly from atomic contributions of the nitramine and ethyl moieties. The LUMO is confined to the nitrato part of NENA. In both orbitals mainly π-type symmetry exists. In the case of anionic form, the α- and β-HOMO spread over the nitrato and nitramine parts, respectively, and the α- and β-LUMO possess reverse location to the HOMOs. On the other hand, in the cationic form the locations of the α- and β-HOMO are over the nitrato, whereas the LUMOs spread over the nitramine part, again having π-type symmetry.
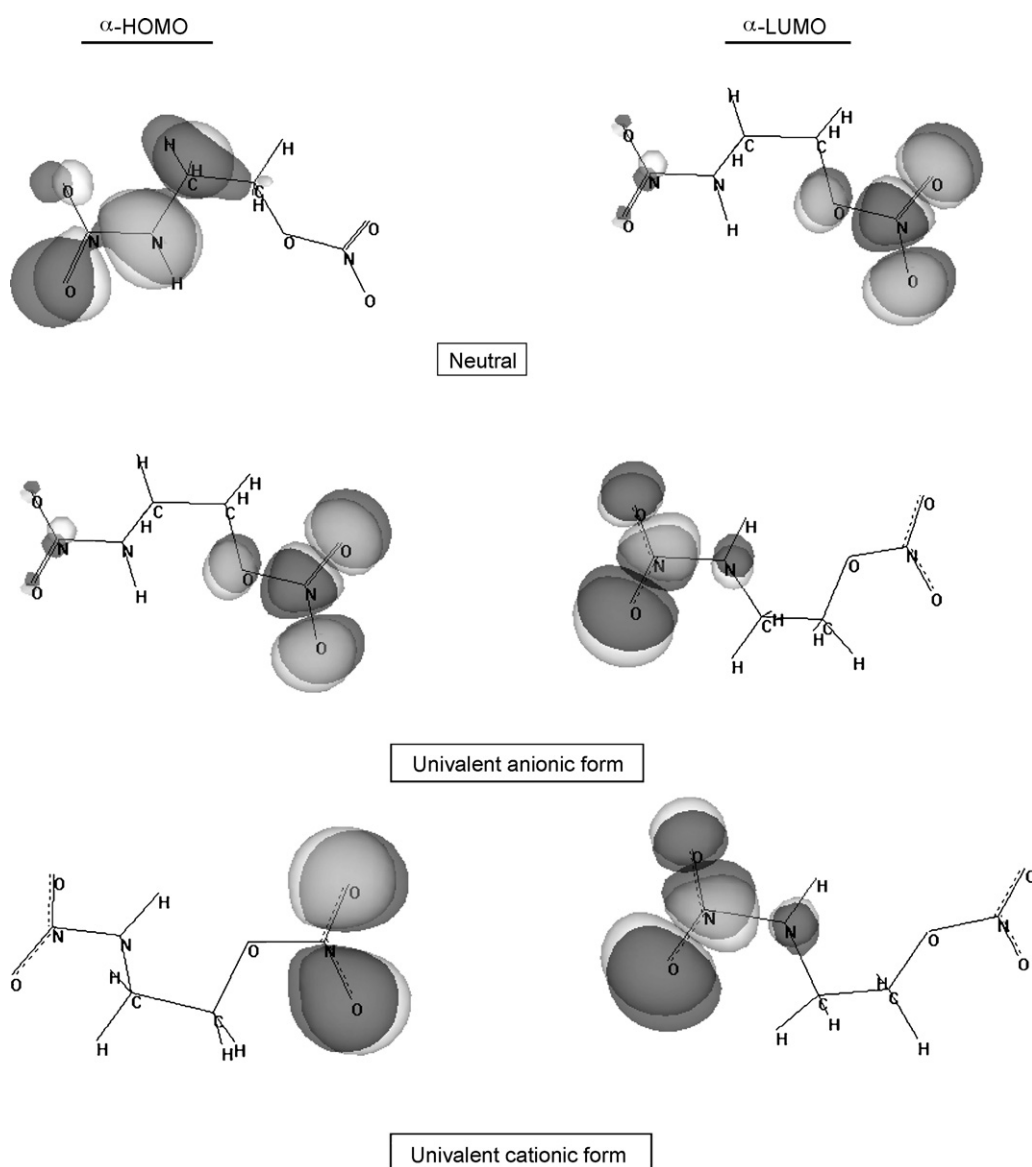
Fig. 6. The frontier molecular orbitals (α-HOMO and α-LUMO) of concerned charged forms. Performed at MP2/6-311G(d,p) single point over UHF/6-311G(d,p) optimized structures.

β-HOMO

β-LUMO

Neutral

Univalent anionic form

Univalent cationic form
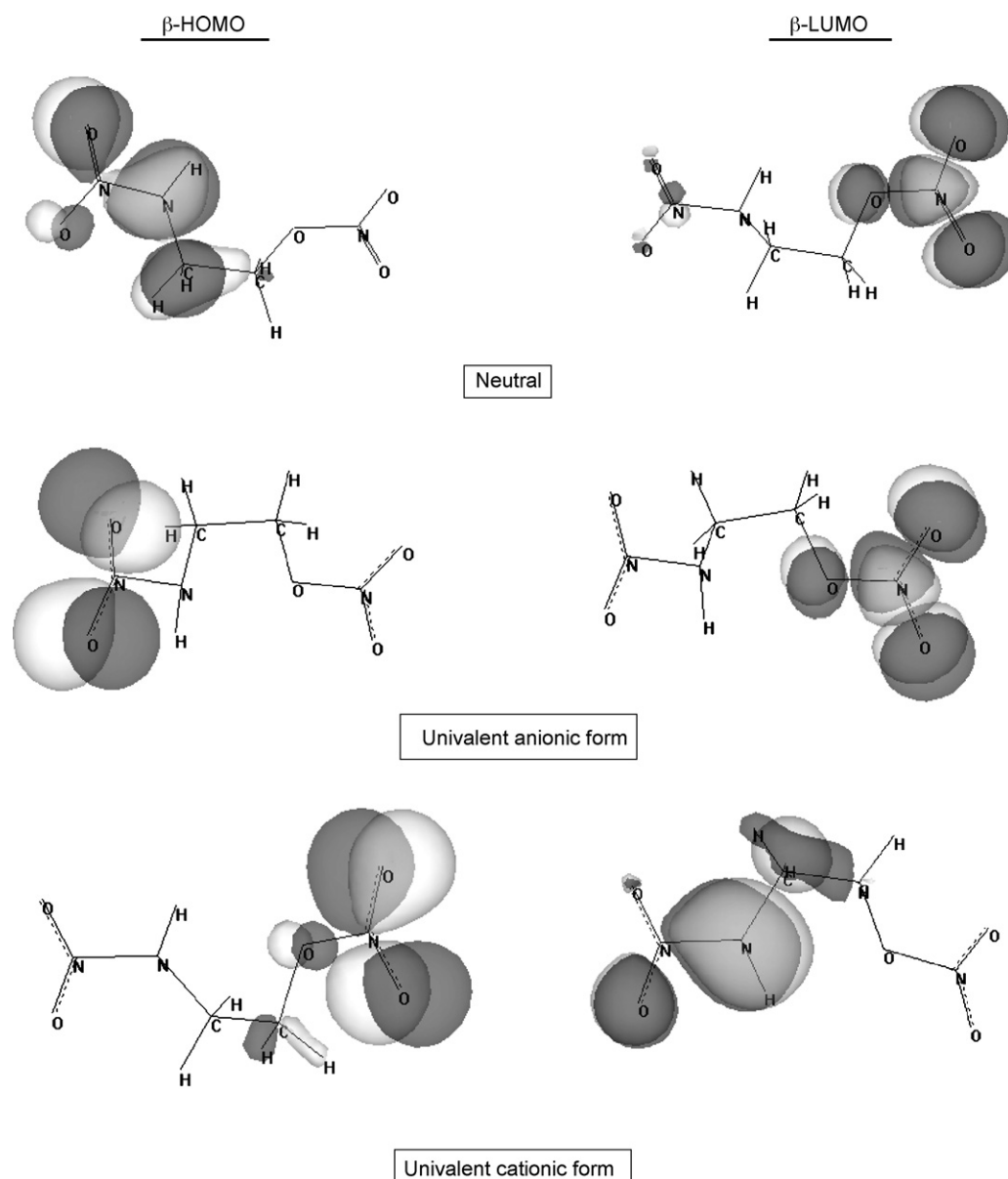
Fig. 7. The frontier molecular orbitals (β-HOMO and β-LUMO) of concerned charged forms. Computed at MP2/6-311G(d,p) single point over UHF/6-311G(d,p) optimized structures.

Table 10
The HOMO and LUMO energies (ε) of the species concerned

Energy	Univalent cation	Neutral	Univalent anion
α-HOMO	−12.597	−8.450	−1.424
β-HOMO	−13.678	−8.450	−1.745
α-LUMO	−7.792	−2.437	2.202
β-LUMO	−10.096	−2.437	1.721
α-$\Delta\varepsilon$	4.805	6.013	3.626
β-$\Delta\varepsilon$	3.582	6.013	3.466

Energies in eV $\Delta\varepsilon = \varepsilon_{LUMO} - \varepsilon_{HOMO}$. Calculated at UB3LYP/6-311G(d,p) level.

Table 11
The HOMO and LUMO energies (ε) of NENA and its tautomers, energies in eV, $\Delta\varepsilon = \varepsilon_{LUMO} - \varepsilon_{HOMO}$

	NENA	T_1	T_2
HOMO	−8.723	−8.416	−8.310
LUMO	−2.799	−2.451	−2.483
$\Delta\varepsilon$	5.924	5.965	5.827

Calculated at B3LYP/6-311+G(d,p) level.

Tables 10 and 11 show the energies of the frontier molecular orbitals of the species of present concern. As seen in Table 10, the cation formation is accompanied by a substantial lowering in the HOMO (α- and β-types) energies as compared to the neutral form. Whereas anion formation causes striking raise of the HOMO. In the case of LUMO energies, the univalent cation is characterized with much lower energy than the neutral form, whereas the anion has highly elevated LUMO energy.

As for the tautomers, the HOMO and LUMO energies conform to the orders of NENA < T_1 < T_2 and NENA < T_2 < T_1, respectively.

Fig. 8 shows the calculated (UB3LYP/6-311+G(d,p) level, unscaled) IR spectra of NENA and its univalent charged forms. As seen there, N—H stretching of these structures occurs in between 3600 and 3400 cm^{-1}. Although, C—H asymmetric stretching is a medium intensity peak in the anion form, it is hardly ever observed in the other spectra. The nitrato N=O asymmetric stretching occurs at 1721, 1988 and 1566 cm^{-1} for the neutral, cation and anion forms, respectively. These peaks overlap with N—H in-plane
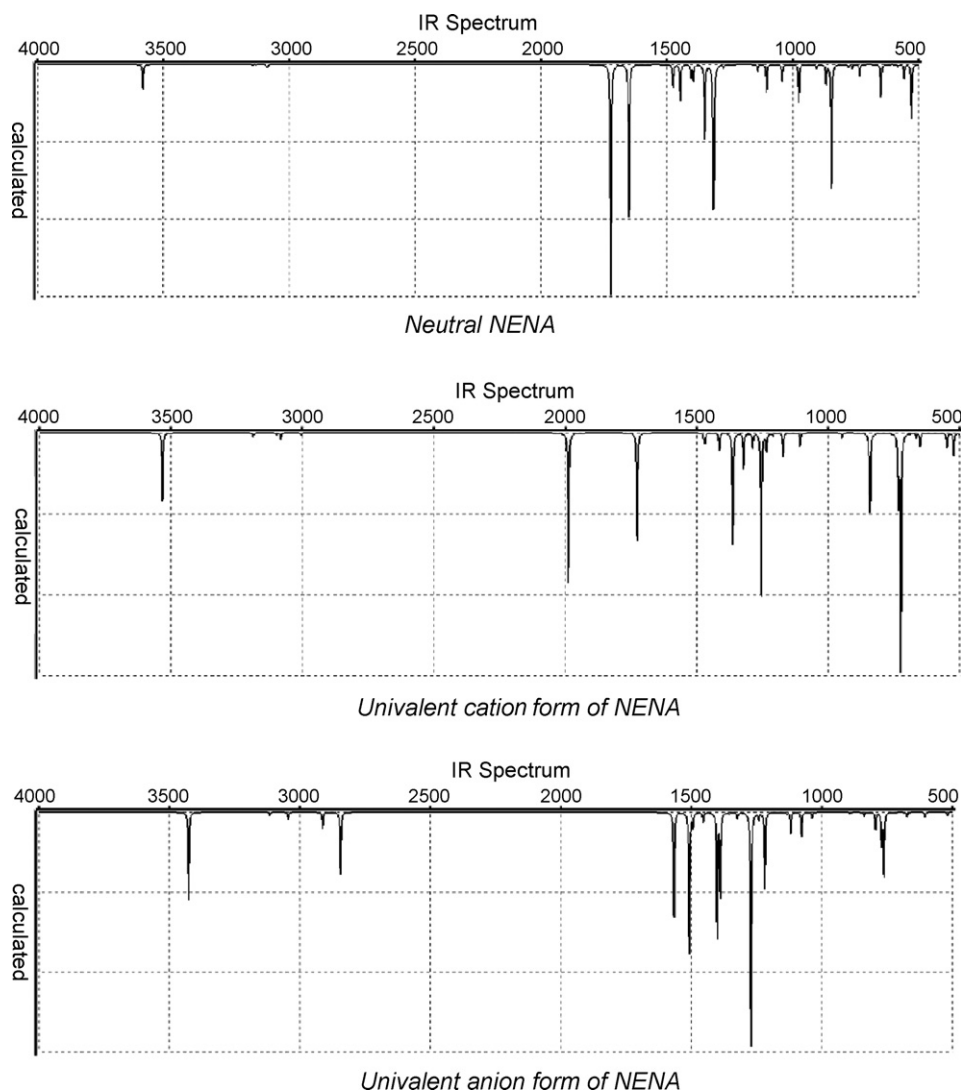
Fig. 8. Calculated IR spectra of concerned species at UB3LYP/6-311+G(d,p) level.

bendings. The O—N (ester) and N—N stretchings appear in the region of 850–700 cm^{-1}, respectively. Up to the best of our knowledge, experimental IR data for any of these structures is not known. The calculated data indicate that the position of ester NO$_2$ and nitramine nitro asymmetric vibrations are very sensitive to charge development.

3.4. Molecular dynamics studies

In explosion type strong exothermic reactions it is almost impossible to maintain isothermal conditions owing to their tendency for self-heating. All of a sudden, the sample is heated to T. At such high temperatures also some ionizations occur. However, the evidence from isothermal and adiabatic decomposition studies indicates that the activation energy may be approximately the same for all normal CHNO explosives. Moreover, it appears to be the same in the detonation reaction as in the much lower temperature thermal decomposition for these explosives [32].

In the present study, a constant temperature molecular dynamics (isothermal quantum dynamics using PM3 method) of NENA has been studied to investigate how stable NENA is at a moderately high temperature. For that purpose, the bath relaxation constant, τ, is set to 0.01 ps. Note that a small number for the bath relaxation

constant results in tight coupling and holds the temperature closer to the chosen temperature.

Presently, the trajectories of all the bonds (except C—H bonds) and their deviations from the mean values were followed. Fig. 9 shows such a study for N—N and N—O bonds of NENA. The molecular dynamics calculations revealed that O3—N4 bond (O—NO$_2$
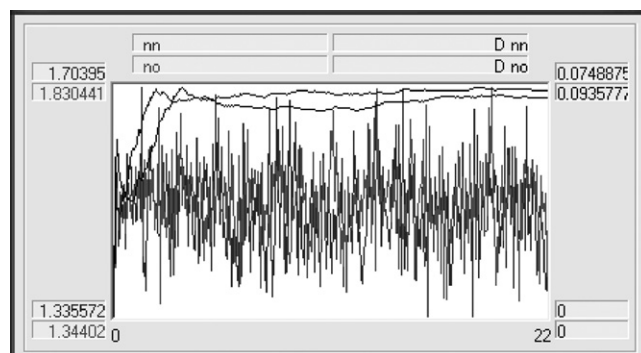

Fig. 9. Trajectory of N—N and N—O bonds and their deviations from the mean (Dnn and Dno values in the figure).

Table 12
The descriptive statistics of certain bonds of NENA in the present MD studies

	C—N	C—O	N—N	N—O
Mean	1.495228	1.411611	1.505303	1.580842
Standard error	0.000199	0.000192	0.000353	0.000428
Median	1.493067	1.40947	1.501797	1.586264
Mode	1.489319	1.387150	1.465901	1.469079
Standard deviation	0.041670	0.040307	0.073968	0.089718
Sample variance	0.001736	0.001625	0.005471	0.008049
Kurtosis	0.239267	0.503922	−0.3342402	−0.215101
Skewness	0.282046	0.401520	0.234757	−0.146060
Range	0.305923	0.323329	0.468861	0.547299
Minimum	1.366871	1.276211	1.289554	1.295223
Maximum	1.672794	1.599540	1.758415	1.842522
Sum	65791.54	62112.29	66234.85	69558.64
Count	44001	44001	44001	44001
Largest (1)	1.672794	1.599540	1.758415	1.842522
Smallest (1)	1.366871	1.276211	1.289554	1.295223
Confidence Level (95.0%)	0.000389	0.000377	0.000691	0.000838
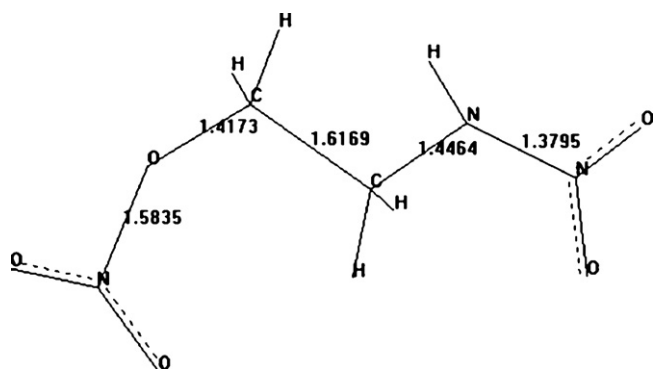
Fig. 10. Snapshot from the trajectory ($t = 21$ ps), PM3 MD calculations (starting geometry was optimized at UB3LYP/6-311G(d,p) level).

bond) undergoes elongation but N—N (nitramine bond) remains almost constant. Fig. 10 displays a snapshot from the trajectory ($t = 21$ ps) indicating the bond lengths. The descriptive statistics (44001 counts) of certain bonds of NENA in the present MD studies are shown in Table 12. As seen in the table, all the distributions are platykurtic [38]. The largest skewness occurs in the distribution of C—O bond lengths. Whereas O—N bond length distribution is characterized with negative skewness and kurtosis. The largest span of bond lengths when NENA exposed to heat is associated with O—NO$_2$ bond (O—N bond in the table) and its largest length is 1.84 Å. Thus, this bond has higher tendency to break down thermally compared to the others. Note that the characteristic values are 1.45–1.47 Å for C—N bonds of nitramines, 1.34–1.38 Å for C—O bonds, 1.38–1.48 Å for nitramine N—N bonds and 1.45–1.51 Å for N—O bonds [39]. Although, modes (most frequently occurred values) of the bond length distributions for these bonds are not very much different than the characteristic values given above, the mean values of N—N and O—N bonds differ than those, indicating that some extreme bond lengths contribute to the mean, e.g., 1.843 Å for O—NO$_2$ bond.

4. Conclusion

Presently performed quantum chemical investigations on NENA showed that of the two NO$_2$ groups present in the structure, the one linked to the ester oxygen is more likely to dissipate than the nitramine NO$_2$ group (either thermally or by negative electric charging). Note that avoidance of static charging of explosive materials has prime importance for the purpose of handling and storage of them, because many unexpected hazards may happen otherwise.

Also present calculations indicate that *s-cis* conformation of NENA is slightly more stable than the *s-trans*. On the other hand, on the basis of homolytic bond dissociation energies for O—NO$_2$ bond in the structures, it is clear that the presence of the tautomers in the bulk of NENA somewhat should decrease its sensitivity.

References

[1] W. Beck, T.M. Klapötke, Mercury fulminate: ONC-Hg-CNO or CNO-Hg-ONC—a DFT study, J. Mol. Struct. (THEOCHEM) 848 (2008) 94–97.
[2] M.J. Huang, J. Leszczynski, The mechanism of the radical-anion reduction of 2,4,6-trinitrotoluene: a theoretical insight, J. Mol. Struct. (THEOCHEM) 593 (2002) 105–113.
[3] C. Zhang, Investigation of correlation between nitro group charges and C-nitro bond strength and amino group effect on C-nitro bonds in planar conjugated molecules, Chem. Phys. 324 (2006) 547–555.
[4] L. Türker, T. Atalar, *Ab initio* and DFT study on 1,4-dinitroglycoluril configurational isomers: *cis*-DINGU and *trans*-DINGU, J. Hazard. Mat. A137 (2006) 47–56.
[5] L. Türker, T. Atalar, Quantum chemical study on 5-nitro2,4-dihydro-3H-1,2,4,triazol-3-one (NTO) and some of its constitutional isomers, J. Hazard. Mat. A137 (2006) 1333–1344.
[6] A. Gindulyte, L. Massa, L. Huang, J. Karle, Ab initio study of unimolecular decomposition of nitroethylene, J. Phys. Chem. A 103 (1999) 11040–11044.
[7] A. Gindulyte, L. Massa, L. Huang, J. Karle, Proposed mechanism of 1,1-diamino-dinitroethylene decomposition: a density functional theory study, J. Phys. Chem. A 103 (1999) 11045–11051.
[8] M.A. Bohn, Determination of the kinetic data of the thermal decomposition of energetic plasticizers and binders by adiabatic self heating, Thermochim. Acta 337 (1999) 121–139.
[9] R.L. Simmons, NENAs–New Energetic Plasticizers, NIMIC-S-275-94, NATO, Brussels, Belgium, 1994.
[10] G.F. Wright, W.J. Chute, Nitramines and their preparation, U.S. Pat. 2,461,582 (1949).
[11] G.F. Wright, W.J. Chute, Method of converting secondary amines to nitramines, U.S. Pat. 2,462,052 (1949).
[12] R.A. Johnson, J.J. Mullay, Stability and performance characteristics of NENA materials and formulations, in: Joint International Symposium on Energetic Materials Technology, New Orleans, LA, 5–7 October, NDIA, 1992.
[13] R.L. Simmons, Thermochemistry of NENA plasticizers, in: 25th Int. Ann. Conf. ICT, Karlsruhe, Germany, June 28–July 1, 1994, pp. 10/1–10/10.
[14] T.K. Chakraborty, K.C. Raha, B. Oprakash, A. Singh, A Study on gun propellants based on butyl-NENA, Energ. Mat. 21 (2004) 41–53.
[15] K. Dudek, P. Marecek, J. Skladal, Z. Jalovy, Synthesis and some properties of Bu-NENA, new trends in research of energetic materials, in: Proceedings of the Seminar, 7th, Pardubice, vol. 2, Czech Republic, April 20–22, 2004, 2004, Meeting date 2004, 464–471.
[16] H.H. Licht, H. Ritter, B. Wanders, NENA explosives, International Annual Conference of ICT, 27th (Energetic Materials) (1996) 28.1–28.10.
[17] V.A. Tartakovskii, A.S. Ermakov, Y.A. Strelenko, D.B. Vinegradov, E.Y. Petrov, New synthetic approaches to functionally substituted 4,5-dihydro-1,2,3-oxadiazole 2-oxides, Russ. J. Org. Chem. 41 (1) (2005) 120–123.
[18] H. Ritter, M.R. Schafer, B. Wanders, H.H. Licht, Synthesis and explosive properties of insensitive energetic NENA explosives, in: Proceedings of the International Pyrotechnics Seminar (1999), 25th (7e Congres International Pyrotechnie du "Groupe de Travail de Pyrotechnie", vol. 1, 1999, pp. 114–122.
[19] L. Anfang, Development of nitroxyethylnitramine plasticizer, Hanneng Cailiao 6 (1) (1998) 43–47.

[20] N. Wingborg, C. Eldsater, 2,2-Dinitro-1,3-bis-nitrooxy-propane (NPN): a new energetic plasticizer, propellants, explosives, Pyrotechnics 27 (2002) 314–319.

[21] H.H. Licht, H. Ritter, NENA compounds as energy carriers in formulations of explosives and powders, in: Proceedings of the International Pyrotechnics Seminar (1999), 25th (7e Congress International de Pyrotechnic du "Groupe de Travail de Pyrotechnie", vol. 1, 1999, pp. 114–122.

[22] M.J. Frisch, G.W. Trucks, H.B. Schlegel, G.E. Scuseria, M.A. Robb, J.R. Cheeseman, J.A. Montgomery Jr., T. Vreven, K.N. Kudin, J.C. Burant, J.M. Millam, S.S. Iyengar, J. Tomasi, V. Barone, B. Mennucci, M. Cossi, G. Scalmani, N. Rega, G.A. Petersson, H. Nakatsuji, M. Hada, M. Ehara, K. Toyota, R. Fukuda, J. Hasegawa, M. Ishida, T. Nakajima, Y. Honda, O. Kitao, H. Nakai, M. Klene, X. Li, J.E. Knox, H.P. Hratchian, J.B. Cross, C. Adamo, J. Jaramillo, R. Gomperts, R.E. Stratmann, O. Yazyev, A.J. Austin, R. Cammi, C. Pomelli, J.W. Ochterski, P.Y. Ayala, K. Morokuma, G.A. Voth, P. Salvador, J.J. Dannenberg, V.G. Zakrzewski, S. Dapprich, A.D. Daniels, M.C. Strain, O. Farkas, D.K. Malick, A.D. Rabuck, K. Raghavachari, J.B. Foresman, J.V. Ortiz, Q. Cui, A.G. Baboul, S. Clifford, J. Cioslowski, B.B. Stefanov, G. Liu, A. Liashenko, P. Piskorz, I. Komaromi, R.L. Martin, D.J. Fox, T. Keith, M.A. Al-Laham, C.Y. Peng, A. Nanayakkara, M. Challacombe, P.M.W. Gill, B. Johnson, W. Chen, M.W. Wong, C. Gonzalez, J.A. Pople, Gaussian 03, Revision B.01, Gaussian Inc., Wallingford, CT, 2004.

[23] W. Kohn, L.J. Sham, Self-consistent equations including exchange and correlation effects, Phys. Rev. 140 (1965) 1133–1138.

[24] R.G. Parr, W. Yang, Density Functional Theory of Atoms and Molecules, Oxford University Press, London, 1989.

[25] J.P. Perdew, Density-functional approximation for the correlation energy 550 of the inhomogeneous electron gas, Phys. Rev. B 33 (1986) 8822–8824.

[26] SPARTAN 06, Wavefunction Inc., Irvine CA, USA.

[27] B.M. Rice, S. Sahu, F.J. Owens, Density functional calculation of bond dissociation energies for NO_2 scission in some nitroaromatic molecules, J. Mol. Struct. (THEOCHEM) 583 (2002) 69–72.

[28] J. Shao, X. Cheng, X. Yang, Density functional calculations of bond dissociation energies for removal of the nitrogen dioxide moiety in some nitroaromatic molecules, J. Mol. Struct. (THEOCHEM) 755 (2005) 127–130.

[29] S.F. Boys, F. Bernardi, The calculation of small molecular interaction by the differences of separate total energies: some procedures with reduced errors, Mol. Phys. 19 (1970) 553–566.

[30] L. Türker, Molecular dynamics and quantum chemical studies on nitroglycerine, J. Mol. Struct. (THEOCHEM) 680 (2004) 53–57.

[31] Hyperchem program, Hypercube, Canada, 1996.

[32] M.A. Cook, The Science of High Explosives, R. E. Krieger Pub. Co. Inc., New York, 1971.

[33] D.K. Cheng, Field and Wave Electromagnetics, Addison-Wesley, Reading, 1983.

[34] P.V. Bharatam, K. Lammertsma, Nitro ↔ aci-nitro tautomerism in high-energetic nitro compounds, in: P.A. Politzer, J.S. Murray (Eds.), Energetic Materials, Part 1: Decomposition, Crystal and Molecular Properties, 12, Elsevier, 2003, pp. 61–89.

[35] S. Zeman, A study of chemical micro-mechanisms of initiation of organic polynitro compounds, in: P.A. Politzer, J.S. Murray (Eds.), Energetic Materials, Part 2: Detonation, Combustion Theoretical and Computational Chemistry, 13, Elsevier, 2003, pp. 25–52.

[36] D. Chakraborty, R.P. Muller, S. Dasgupta, W.A. Goddard, The mechanism for unimolecular decomposition of RDX (1,3,5-trinitro-1,3,5-triazine), an *ab initio* study, J. Phys. Chem. A 104 (2000) 2261–2272.

[37] S.W. Zhang, T.N. Truong, Thermal rate constants of the NO_2 fission reaction of gas phase α-HMX: a direct *ab initio* dynamics study, J. Phys. Chem. A 104 (2000) 7304–7307.

[38] R.R. Sokal, F.J. Rohlf, Biometry, Freeman Pub., New York, 1981.

[39] L.V. Vilkov, V.S. Mastryukov, N.I. Sadova, Determination of the Geometrical Structure of Free Molecules, Mir Publishers, Moscow, 1983.